

# Interfacial microstructure of SiCp/Al composite produced by the pressureless infiltration technique

Qiang Zhang\*, Xiangyu Ma, Gaohui Wu

*School of Materials Science and Engineering, Harbin Institute of Technology, Harbin 150001, China*

Received 10 October 2012; received in revised form 20 November 2012; accepted 25 November 2012

Available online 3 December 2012

## Abstract

A SiCp/Al composite was fabricated by the pressureless infiltration of an Al–Mg–Si alloy into the pre-oxidized SiC preform at 1000 °C for one hour. The composite fully infiltrated and a homogenous distribution of SiC particles was confirmed. MgAl<sub>2</sub>O<sub>4</sub> was found as the interfacial reaction product, its formation deriving from the reactions:  $2\text{Mg} + \text{SiO}_2 = 2\text{MgO} + \text{Si}$  and  $2\text{MgO} + 4\text{Al} + 3\text{SiO}_2 = 2\text{MgAl}_2\text{O}_4 + 3\text{Si}$ . The factors influencing the spontaneous infiltration process were also discussed.

© 2012 Elsevier Ltd and Techna Group S.r.l. All rights reserved.

**Keywords:** B. Composites; Pressureless infiltration; Interfacial reactions; Reactive wetting

## 1. Introduction

Due to the outstanding specific strength and modulus, improved wear-resistance, tailorable thermo-physical properties and flexible fabrication process, the SiCp/Al composites have played a vital role in various areas, such as space, aerospace, transportation or electronic systems [1–4]. The SiCp/Al composites can be produced by the molten aluminum infiltration techniques, such as pressure assisted, vacuum driven and pressureless or capillarity driven process. Aghajanian and co-workers [5,6] first reported the pressureless infiltration technique, by which the aluminum alloys infiltrated the SiC particles preforms spontaneously in a nitrogen atmosphere. This method is believed to be a cost-effective, nearly-net shape technique with combined processing of materials and shaping of components simultaneously [7,8].

During the pressureless infiltration process of SiCp/Al composites, the pre-oxidation of SiC particles has often been used to improve the wetting between SiC and aluminum matrix. In the present work, the SiC particles were pre-oxidized and then the SiCp/Al composite was produced using a spontaneous infiltration technique. The

composite was obtained at higher temperatures (1000 °C) for relatively longer duration (one hour) compared to those produced by the pressure assisted or vacuum driven process; hence the emphasis of this work was focused on the thorough examination of interfacial microstructures. The factors influencing the spontaneous infiltration process were also discussed.

## 2. Experimental

### 2.1. Preparation of the preform

The reinforcement is the  $\alpha$ -SiC particle with an average diameter of 10  $\mu\text{m}$ . The particles were pre-oxidized at 1100 °C for 4 h to remove the impurities and introduce a silica layer on the particle surfaces. The formation of silica layer helps to improve the wettability of SiC by aluminum [9].

The SiC particles were first mixed with the polyvinyl alcohol (PVA), poured into a mold cavity and pressed into the required density by the mechanical pressing. The green samples, 45 mm  $\times$  15 mm  $\times$  8 mm in size, were heated to 400 °C at 5 °C/min to burn out the PVA binder. Then they were heated to 1100 °C and held for 2 h to get enough strength for handling in the following infiltration stage. The processes were carefully controlled to avoid changing

\*Corresponding author. Tel.: +86 451 86402373x5052;  
fax: +86 451 86412164.

E-mail address: [zhang\\_tsiang@hit.edu.cn](mailto:zhang_tsiang@hit.edu.cn) (Q. Zhang).

the shape and dimensions of the preform or introducing micro-cracks.

## 2.2. Fabrication of the composite

The matrix used in the present study is an Al–Mg–Si series alloy. During the infiltration process, the matrix billet and sintered SiC preform (45% volume fraction) were heated to 1000 °C for one hour in an alumina tube furnace with flowing pure N<sub>2</sub> to let the matrix alloy infiltrate the preform pressurelessly. After infiltrated, the samples were removed from the furnace and the SiCp/Al composite was obtained.

## 2.3. Characterization

A HITACHI S-4700 scanning electron microscope (SEM) was used to examine the microstructure of SiCp/Al composite and the morphology of SiC particles. The

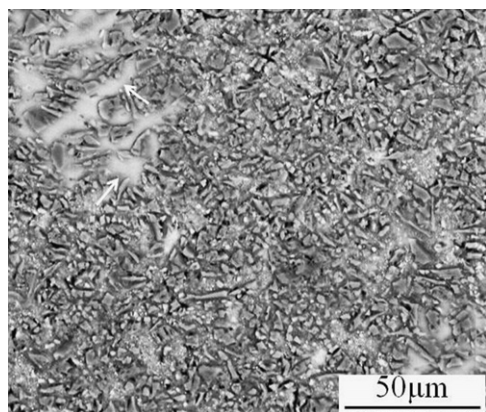


Fig. 1. Backscattering electron image of SiCp/Al composite.

XRD analysis was performed on a D/max-B diffractometer (Rigaku, Japan) at a rate of 0.02° per 0.5 s in step-scan mode using monochromated Cu K $\alpha$  radiation ( $\lambda=0.15405$  nm). The TEM and HREM microstructure observations were carried out on a Philips TECNAI-20 transmission electron microscope and JEOL-2010F high-resolution transmission electron microscope, respectively, operated at 200 kV. The samples for TEM observations were prepared by mechanical polishing, punching, and ion thinning using a Gattan-600 ion beam thinning machine.

## 3. Results and discussion

### 3.1. Microstructure of the SiCp/Al composite

Fig. 1 shows the backscattering electron image of the composite. The SiCp/Al composite fully infiltrates and no matrix-rich channels are found. The SiC particles appear to be uniformly distributed, without any particles clustering. The uniform distribution of reinforcement particles is beneficial to reduce the stress concentration and enhance the load-bearing ability of the composite. The measured density of the SiCp/Al composite is 2.79 g/cm<sup>3</sup>. By comparing the measured density with the theoretical value, a retained porosity of 1.4% is obtained for the composite. The closed micro-cavities in the sintered preform might be the source of retained pores in the composite.

Some white block-like phases are found in Fig. 1, as indicated by the arrows. To identify these phases, the area distribution of element Si, C, Al, Mg and O was analyzed and shown in Fig. 2. As can be seen, these white bulks correspond to the Si phases, resulting from the solidified primary Si phases of the Al–Mg–Si matrix alloy. In Fig. 2(e), the element Mg is found to be segregated. The element O shows a similar distribution, suggesting the

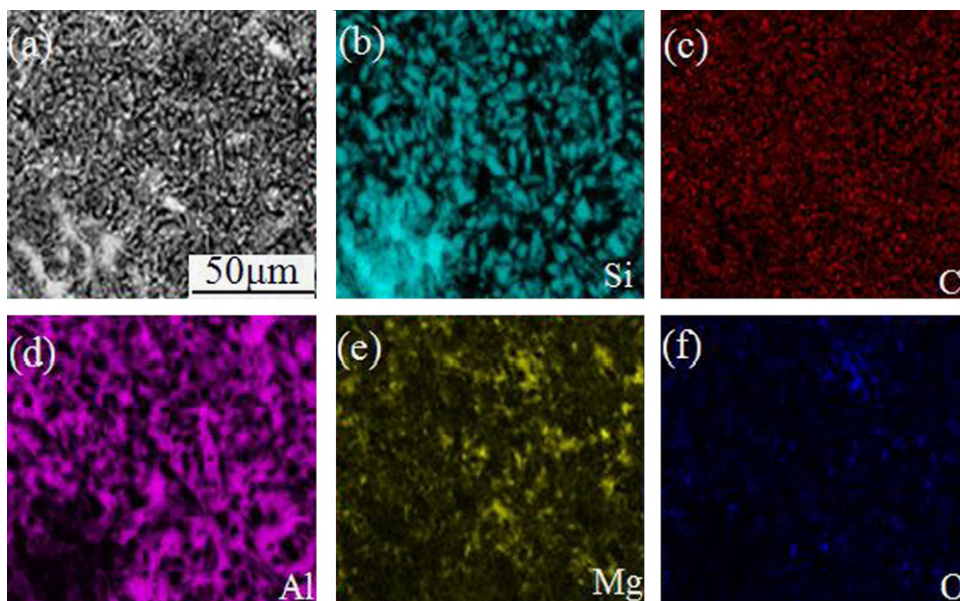


Fig. 2. Microstructure (a) and corresponding area distribution analysis of Si (b), C (c), Al (d), Mg (e) and O (f) in SiCp/Al composite.

existence of some possible interfacial reaction products with Mg and O.

### 3.2. Interfacial microstructure

To determine the interfacial reaction product and observe its morphology, the SiC particles were extracted from the SiCp/Al composite. The solution was mixed with acids containing HF, HCl and HNO<sub>3</sub>. The composite was immersed into the acid solution for 5 h to extract enough particles. Then the SiC particles with reaction products were cleaned and dried rapidly for the following XRD analysis and SEM observation.

Fig. 3 is the XRD result for the SiC particles extracted from the composite. The existences of SiC and MgAl<sub>2</sub>O<sub>4</sub> are confirmed, coming from the reinforcements and interfacial reaction products, respectively. Fig. 4 describes the SEM morphology of the oxidized and extracted SiC particles. The oxidized SiC particles have clean surfaces and clear edges. However, some block-like interfacial reaction products are found in the extracted particles (as shown in Fig. 4(b)), distributing discretely on the particle surface. The EDS analysis in the cross position in Fig. 4(b) is given in Fig. 4(c), indicating that the main elements of these discrete blocks are O, Mg, Al and Si. The O, Mg, Al come from the

interfacial reaction product, and the existence of Si probably results from the SiC particle under the reaction product.

Fig. 5 shows the TEM microstructure of the SiCp/Al composite. Polyhedral interfacial reaction products are found. The EDS analysis in Fig. 5(b) suggests that their major elements are O, Mg and Al, and they are designated as MgAl<sub>2</sub>O<sub>4</sub> according to the diffraction pattern result in Fig. 5(c). A HREM image demonstrating the sophisticated interfacial features is given in Fig. 6, where the spinel phase MgAl<sub>2</sub>O<sub>4</sub> is at the bottom of the image, and the SiC, at the top. The orientation index of [341] in SiC is parallel to the injection electron beams, and the angle between (1 $\bar{1}$ 01) SiC and (1 $\bar{1}$  $\bar{1}$ ) MgAl<sub>2</sub>O<sub>4</sub> is about 17°. It is found that the spinel MgAl<sub>2</sub>O<sub>4</sub>/SiC interface is clean and free from other phases. The interface shows good bonding condition, which is favorable to the mechanical properties of the SiCp/Al composite.

### 3.3. Formation of interfacial reactions

It has been found that there is an incubation period during the infiltration process [10], only after which the molten aluminum can penetrate the SiC preform pressurelessly. Previous results [11–13] indicated that a tenacious alumina film would be developed on the aluminum surfaces. The formation of  $\gamma$ -Al<sub>2</sub>O<sub>3</sub> was confirmed even at an oxygen partial pressure of  $\sim 0.5 \times 10^{-7}$  bar at 475 °C [14]. The alumina film prevented the direct contact of molten aluminum with the preform. In the present work, the high-purity N<sub>2</sub> has about  $3 \times 10^{-5}$  bar oxygen. The aluminum surface invariably had a film of alumina. By using Al–Mg series alloy, for one thing, Mg would react with Al<sub>2</sub>O<sub>3</sub> to form MgO on the surface of molten aluminum. One hour heat treatment of Al–2.5% Mg alloy in the flowing air at 500 °C was sufficient to ensure no significant coverage of alumina at the free surface [13]. Besides, Mg is surface active and has a very high vapor pressure, and then is easy to evaporate from the liquid alloy. Then the

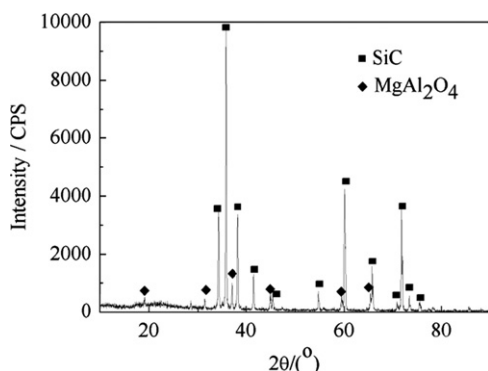


Fig. 3. XRD result of SiC particles extracted from composite.

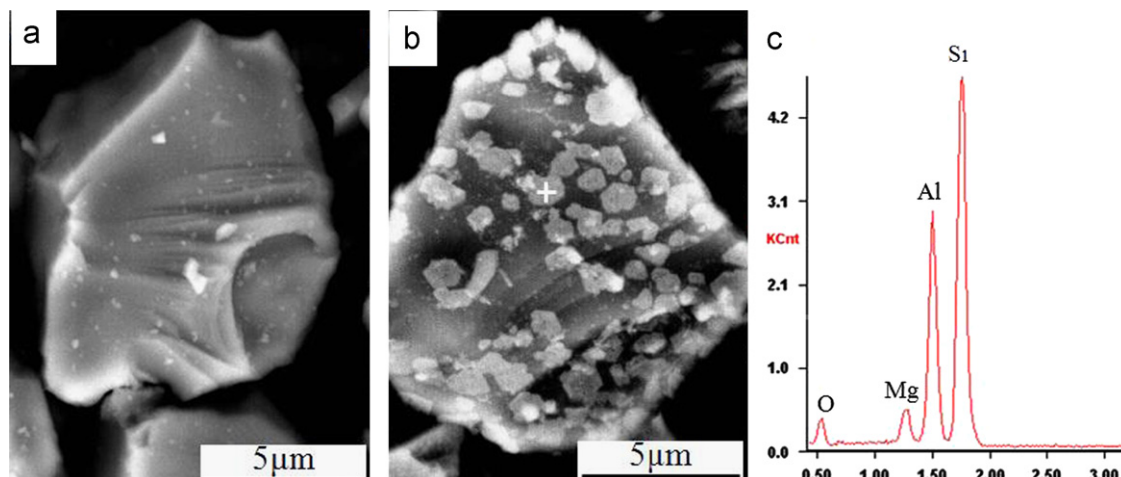


Fig. 4. SEM morphology of SiC particles: (a) oxidized particles, (b) particles extracted from composite and (c) EDS analysis.



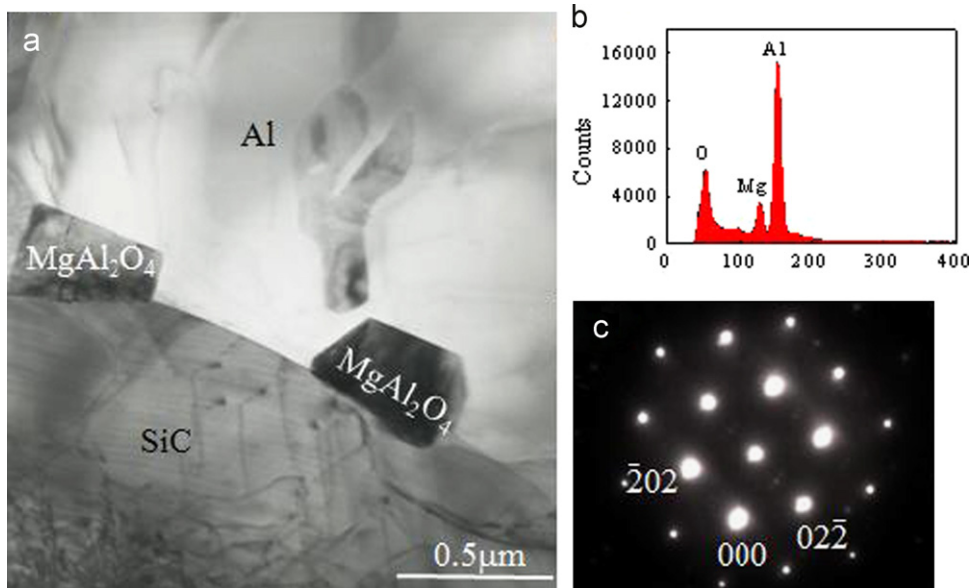


Fig. 5. TEM micrographs of SiCp/Al composite. (a) TEM microstructure, (b) EDS analysis and (c) SADP of [111]MgAl<sub>2</sub>O<sub>4</sub>.

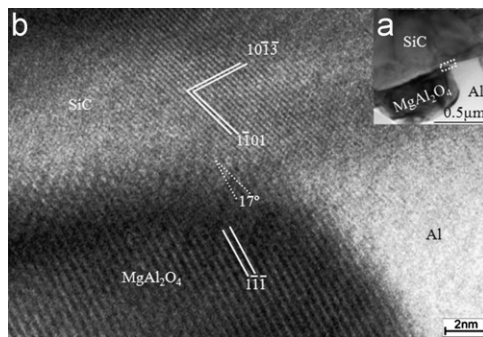


Fig. 6. HREM image of SiCp/Al composite.

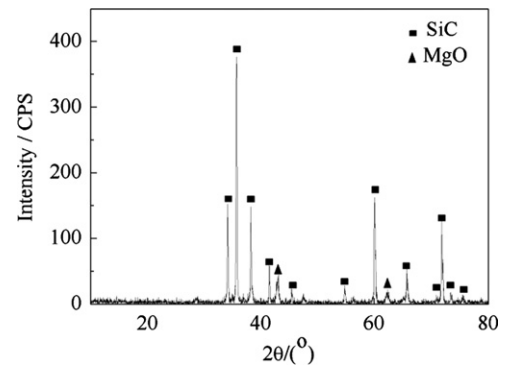


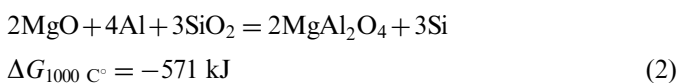
Fig. 7. XRD result of un-infiltrated SiC particles.

alumina film was broken up, leading to the channels for the liquid penetration.

In the samples taken out of the furnace during the incubation period, it was found that the SiC preform kept un-infiltrated and turned to be light yellow from original green. The XRD result of the un-infiltrated SiC particles is shown in Fig. 7. The existences of SiC and MgO indicate that the Mg reacted with the SiO<sub>2</sub> layer to form MgO during the incubation period, according to the reaction (1). The reaction product of MgO remained on the surface of SiC particles.



However, only the MgAl<sub>2</sub>O<sub>4</sub>, instead of MgO, was found at the interfaces of SiCp/Al composite. MgO is unstable when the molten Al and SiO<sub>2</sub> also exist. They can react further to form MgAl<sub>2</sub>O<sub>4</sub> during the infiltration process, as shown in (2). It is favorable thermodynamically, leading to the final formation of MgAl<sub>2</sub>O<sub>4</sub>.



In the reactive metal-ceramics system, the contact angle  $\theta$  is given by [15]:

$$\cos\theta = \cos\theta_0 - \frac{\Delta\sigma_r}{\Delta\sigma_{LV}^0} - \frac{\Delta G_r}{\Delta\sigma_{LV}^0} \quad (3)$$

where  $\cos\theta_0$  and  $\sigma_{LV}^0$  is the contact angle and liquid surface tension in the absence of reactions,  $\Delta\sigma_r$  is the change in interfacial tension brought about by the interfacial reaction, and  $\Delta G_r$  is the change in free energy per unit area released by reactions.

Interfacial reactions will result in a net decrease of the free energy, namely  $\Delta G_r < 0$ , otherwise, the reactions will not proceed. Aksay [16] et al. studied the variation of dynamic interfacial tension with time during a chemical reaction between two phases. The chemical reactions at the interface initially lead to a decrease in the corresponding interfacial tension. After the completion of interfacial reactions followed by the continuation into the bulk regions by diffusion, the interfacial tension gradually increases toward their static value which is still lower than

the original value, namely,  $\Delta\sigma_r < 0$ . Therefore, with the combined effects of  $\Delta G(t)$  and  $\Delta\sigma(t)$ , the  $\cos\theta(t)$  will be increased and a decreased wetting angle is obtained. The interfacial reactions would lead to a decrease in the dynamic wetting angle between reinforcement particles and matrix [17,18]. Then the formation of  $\text{MgAl}_2\text{O}_4$  improved the wetting between the SiC and matrix. Additionally, the element Mg diminished the surface tension of molten aluminum [19] and the element Si increased its fluidity. Both would promote the pressureless infiltration process. With the continuous infiltration, the fully-infiltrated and dense SiCp/Al composite was obtained.

#### 4. Conclusions

By using oxidized SiC particles, the SiCp/Al composite was fabricated by the pressureless infiltration technique.  $\text{MgAl}_2\text{O}_4$  was found as interfacial reaction product, its formation deriving from the reactions:  $2\text{Mg} + \text{SiO}_2 = 2\text{MgO} + \text{Si}$  and  $2\text{MgO} + 4\text{Al} + 3\text{SiO}_2 = 2\text{MgAl}_2\text{O}_4 + 3\text{Si}$ . The interfacial reactions enhanced the wettability and promoted the spontaneous infiltration process.

#### Acknowledgment

The authors gratefully acknowledge the financial support from the Fundamental Research Funds for the Central Universities (Grant no. HIT.NSRIF.2013003).

#### References

- [1] A.M. Zahedi, J. Javadpour, H.R. Rezaie, Mehdi Mazaheri, The effect of processing conditions on the microstructure and impact behavior of melt infiltrated Al/SiCp composites, *Ceramics International* 37 (2011) 3335–3341.
- [2] K. Kaur, R. Anant, O.P. Pandey, Tribological behaviour of SiC particle reinforced Al–Si Alloy, *Tribology Letters* 44 (2011) 41–58.
- [3] A. Kalkanli, S. Yilmaz, Synthesis and characterization of aluminum alloy 7075 reinforced with silicon carbide particulates, *Materials and Design* 29 (2008) 775–780.
- [4] M.K. Aghajanian, C.A. Andersson, R.J. Wiener, B.R. Rossing, High-reinforcement-content metal matrix composites, *Automotive Engineering International* 103 (1995) 83–85.
- [5] M.K. Aghajanian, J. Burke, D.R. White, A. Nagelberg, A new infiltration process for the fabrication of metal matrix composites, *Sampe Quarterly* 20 (1989) 43–46.
- [6] M.K. Aghajanian, M.A. Rocazella, J.T. Burke, S.D. Keck, The fabrication of metal matrix composites by a pressureless infiltration technique, *Journal of Materials Science* 26 (1991) 447–454.
- [7] A.M. Zahedi, H.R. Rezaie, J. Javadpour, Mehdi Mazaheri, M.G. Haghighi, Processing and impact behavior of Al/SiCp composites fabricated by the pressureless melt infiltration method, *Ceramics International* 35 (2009) 1919–1926.
- [8] S. Ren, X. Qu, J. Guo, X. He, M. Qin, X. Shen, Net-shape forming and properties of high volume fraction SiCp/Al composites, *Journal of Alloys and Compounds* 484 (2009) 256–262.
- [9] V. Laurent, D. Chatain, N. Eustathopoulos, Wettability of  $\text{SiO}_2$  and oxidized SiC by aluminium, *Materials Science and Engineering A* 135 (1991) 89–94.
- [10] M. Rodriguez-Reyes, M.I. Pech-Canul, E.E. Parras-Medecigo, A. Gorokhovskiy, Effect of Mg loss on the kinetics of pressureless infiltration in the processing of Al–Si–Mg/SiCp composites, *Materials Letters* 57 (2003) 2081–2089.
- [11] B. Srinivasa Rao, V. Jayaram, Pressureless infiltration of Al–Mg based alloys into  $\text{Al}_2\text{O}_3$  preforms: mechanisms and phenomenology, *Acta Materialia* 49 (2001) 2373–2385.
- [12] M. Zayan, O. Jamjoom, N. Razik, High-temperature oxidation of Al–Mg alloys, *Oxidation of Metals* 34 (1990) 323–333.
- [13] C. Lea, J. Ball, The oxidation of rolled and heat treated Al–Mg alloys, *Applied Surface Science* 17 (1984) 344–362.
- [14] G. Scamans, E. Butler, In situ observations of crystalline oxide formation during aluminum and aluminum alloy oxidation, *Metallurgical and Materials Transactions A* 6 (1975) 2055–2063.
- [15] N. Eustathopoulos, A. Mortensen, Capillary phenomena, interfacial bonding, and reactivity, in: S. Suresh, A. Mortensen, A. Needleman (Eds.), *Fundamentals of Metal-matrix Composites*, Butterworth-Heinemann, Stoneham, 1993, pp. 43–60.
- [16] I.A. Aksay, C.E. Hoge, J.A. Pask, Wetting under chemical equilibrium and nonequilibrium conditions, *Journal of Physical Chemistry* 78 (1974) 1178–1183.
- [17] Y.V. Naidich, Y.N. Chubashov, N. Ishchuk, V. Krasovskii, Wetting of some nonmetallic materials by aluminum, *Powder Metallurgy and Metal Ceramics* 22 (1983) 481–483.
- [18] C. Marumo, J.A. Pask, Reactions and wetting behaviour in the aluminium-fused silica system, *Journal of Materials Science* 12 (1977) 223–233.
- [19] C. Garcia-Cordovilla, E. Louis, A. Pamies, The surface tension of liquid pure aluminium and aluminium–magnesium alloy, *Journal of Materials Science* 21 (1986) 2787–2792.